STU
FCHPT

Two tetranuclear [Ni(II)/Dy(III)]$_2$ solvatomorphs based on symmetric bicompartmental Schiff base type ligand

Lenka Krešáková, Juraj Černák

Department of Inorganic Chemistry, Faculty of Science, P. J. Šafárik University in Košice, Moyzesova 11, 041 54 Košice, Slovakia
lenka.kresakova@upjs.sk

Abstract: From the system [Ni(*o-van-en*)] — $DyBr_3$, a novel tetranuclear complex [Ni(*o-van-en*)$Dy(H_2O)_2(OH)]_2Br_4 \cdot 6H_2O$ (**1**) was isolated; H_2(*o-van-en*) was synthesized by 2/1 condensation of *o*-vanillin and ethylenediamine. Single crystals (SC) of **1**, upon standing in methanol/isopropanol mother liquor, underwent a SC-SC transformation and yielded a new solvatomorph [Ni(*o-van-en*)$Dy(H_2O)_2(OH)]_2Br_4 \cdot MeOH \cdot$ *i*$PrOH \cdot H_2O$ (**2**). Both complexes, **1** and **2**, were characterized by elemental analysis, infrared spectroscopy, and single crystal X-ray analysis. Crystal structures of both **1** and **2** are ionic. Within the bicompartmental unit {Ni(*o-van-en*)$Dy(H_2O)_2(\mu$-OH)}, the square coordinated Ni(II) atom occupies the smaller cavity (donor set is *cis*-N_2O_2) while the octacoordinated Dy(III) atom (donor set is O_8) is placed in the larger cavity. The two [Ni(*o-van-en*)$Dy(H_2O)_2(\mu$-OH)] units are linked by a pair of μ-OH bridging ligands. The unit cell content is completed by bromide anions and water (**1**) or methanol, isopropanol, and water solvate molecules (**2**).

Keywords: crystal structure analysis, heterometallic complex, Schiff base type ligand, tetranuclear complex

Introduction

In recent years, the well-known multidentate salen-type ligands have been successfully used to stabilize lanthanide ions in various coordination environments (Tsantis et al., 2019). Specifically, polynuclear Schiff base complexes have proven to be notably distinct luminescent complexes (Hardy et al., 2017) as well as single molecule magnets (SMMs) (Chandrasekhar et al., 2013). Attention has been focused on the crystal structures and magnetic properties of Dy(III) complexes. Vignesh et al. (2017) examined the impact of ligand environment around the Dy(III) atom on SMM behavior, as well as the role and significance of the diamagnetic ions, especially their ability to alter the relaxation process. A family of tetranuclear Co(II)/Ln(III) (Ln(III) = Tb, Dy, Ho) complexes belonging to "butterfly complexes" were characterized. Magnetic study of $[Co_2Dy_2(\mu_3\text{-OH})_2$(*o*-tol)$_4$(mdea)$_2(NO_3)_2]$ (*o*-tol = *o*-toluate, H_2(mdea) = *N*-methyldiethanolamine; KASJAS) (Vignesh et al., 2017) has revealed SMM behavior in the absence of an external field, with U_{eff} of 81.2 cm^{-1}. For previously reported Co_2/Ln_2 butterfly complexes (Langley et al., 2013; Langley et al., 2015), the influence of the Ln(III) coordination sphere modification on the final magnetic properties was studied. A search in the Cambridge Structural Database (CSD) (Groom et al., 2016) revealed 175 hits for *Tr*/Dy complexes (*Tr* refers to a transition metal). Further, a search for structures comprising the *Tr*-O-Dy-$(O)_2$-Dy-O-*Tr* fragment yielded 46 results. These can be divided into six groups considering the presence of the 3*d* atom: **Mn/Dy** (3 hits); **Fe/Dy** (4 hits), **Co/Dy** (8 hits); **Ni/Dy** (6 hits); **Cu/Dy** (3 hits) and **Zn/Dy** (22 hits). Tetranuclear Ni(II)/Dy(III) complexes are summarized in Table 1. Most of the above-mentioned complexes are examples of magnetically active compounds, mostly SMMs. Wu et al. (2017) observed a trend in magnetic interactions when comparing Co_2/Dy_2 complex with an Ni_2/Dy_2 analogue, $[Ni_2Dy_2(Hhms)_2(OAc)_6(MeOH)_2(H_2O)_2] \cdot (NO_3)_2$ (H_2hms = 1-(2-hydroxy-3-methoxybenzylidene)-semicarbazide; VAYNIV) (Tab. 1). The Ni_2/Dy_2 analogue showed longer relaxation time and absence of quantum tunnelling of magnetization at low temperatures; ferromagnetic exchange led to coupling between Ni(II) and Dy(III) atoms (Wu et al., 2017). Using compartmental Schiff base ligand in conjunction with auxiliary ligands, a series of Ni_2/Ln_2 complexes were prepared by Jiang et al. (2017). Tetranuclear structures can be considered as two Ni/Ln dinuclear subunits bridged by two carbonates derived from atmospheric carbon dioxide, i.e. $[(\mu_3\text{-}CO_3)_2${Ni(H*L*2)(EtOH)Dy(OAc)}$_2] \cdot 2$EtOH (H_3L2 = *N*,*N*′-bis(3-methoxysalicylidene)-1,3-diamino-2-propanol); JASTUV01) (Jiang et al., 2017).

Our previous work on dinuclear 3*d*/4*f* complexes (Krešáková et al., 2025; Vráblová et al., 2019) has introduced bottom-up synthesis of these types of complexes based on compartmental multidentate ligands. Preparation of compound **1** in

Tab. 1. List of tetranuclear complexes with $[NiO_2DyO_2DyO_2Ni]$ core upon CSD (version 5.43 update (Nov 2022)) (Groom et al., 2016).

Complex	Refcode	Donor set Ni(II)	Donor set Dy(III)	Reference
$[Ni_2Dy_2(L1)_2(o\text{-van})_2(CO_3)_2(NO_3)_2(MeOH)_2]$	GACQUZ	NO_5	O_9	Upadhyay et al., 2016
$[(\mu_3\text{-}CO_3)_2\{Ni(HL2)(EtOH)Dy(OAc)\}_2]\cdot 2EtOH$	JASTUV01	N_2O_4	O_8	Jiang et al., 2017
$[Ni_2Dy_2(Hhms)_2(OAc)_6(MeOH)_2(H_2O)_2]\cdot(NO_3)_2$	VAYNIV	NO_5	O_9	Wu et al., 2017
$[(\mu_4\text{-}CO_3)_2\{Ni(L3)(H_2O)Dy(NO_3)\}_2]\cdot 2MeCN\cdot 2H_2O$	WIMDED	N_2O_4	O_9	Sakamoto et al., 2013
$[(\mu_4\text{-}CO_3)_2\{Ni(L3)(MeOH)Dy(NO_3)\}_2]$	WIMDUT	N_2O_4	O_9	Sakamoto et al., 2013
$2[(\mu_4\text{-}CO_3)_2\{NiDy(L4)(MeOH)(OAc)\}_2]\cdot 9H_2O\cdot 8MeOH$	XOYLUU	N_2O_4	O_9	Cristovao et al., 2015

Additional text: **H*L1*** = 2-methoxy-6-[(*E*)-phenyliminomethyl] phenol;
H_3*L2* = *N,N´*-bis(3-methoxysalicylidene)-1,3-diamino-2-propanol);
OAc = acetato; **H_2hms** = 1-(2-hydroxy-3-methoxybenzylidene)-semicarbazide;
H_2*L3* = *N,N´*-bis(3-methoxysalicylidene)-1,3-diaminopropane);
H_2*L4* = *N,N´*-bis(5-bromo-3-methoxysalicylidene)propylene-1,3-diamine.

microcrystalline form was performed according to the published approach described previously (Krešáková et al., 2025). As for the crystals' preparation, methanol/isopropanol solvent system in closed vials was chosen with two different types of crystals grown. Herein, a new tetranuclear complex $[Ni(o\text{-}van\text{-}en)Dy(H_2O)_2(OH)]_2Br_4\cdot 6H_2O$ (**1**) and its solvatomorph $[Ni(o\text{-}van\text{-}en)Dy(H_2O)_2(OH)]_2Br_4\cdot MeOH\cdot iPrOH\cdot H_2O$ (**2**) formed via SC-SC transformation are reported.

Material and Methods

Chemicals

Ethylenediamine (≥99.5 %), *o*-vanillin (99 %), $NiCO_3$ (basic hydrate, 46 % as Ni) $DyBr_3\cdot xH_2O$ (p. a.), ethanol (99.8 %), acetone (99.5 %), diethyl ether (99.0 %), isopropanol (99.5 %) were purchased from commercial sources and used as received.

Synthesis of Schiff base ligand H_2(o-van-en)

Ligand H_2(*o-van-en*) was synthesized by a modification of previously reported methods (Andruh, 2015; Vráblová et al., 2019). To the ethanolic solution (50 ml) of *o*-vanillin (0.4542 g, 3 mmol) was added ethylenediamine (0.1 ml, 1.5 mmol). The mixture was refluxed for 5 hours in a boiling flask, and the obtained solution was filtered and left aside to crystallize at room temperature. Dark yellow crystals of the product appeared overnight. The crude product was filtered and washed with a small amount of diethylether. Yield: 90 %.

Anal. [%], calculated for H_2(*o-van-en*), $C_{18}H_{20}N_2O_4$: C, 65.83; H, 6.15; N, 8.53; found: C, 66.05; H, 6.23; N, 8.58.

FT-IR [cm^{-1}]: 3726vw, 2997w, 2931w, 2835w, 2359w, 1630s, 1462s, 1438m, 1408m, 1325w, 1295w, 1244vs, 1189m, 1133m, 1079s, 1049m, 1009m, 987m, 961s, 836s, 791s, 781s, 728s, 620s, 522m, 441m.

^{1}H NMR [ppm]: 3.76s (6H), 3.92s (4H), 6.77—6.80t (2H), 6.99—7.00d (2H), 7.00—7.02d (2H), 8.57s (2H), 13.54s (2H).

^{13}C NMR [ppm]: 55.63 (OCH3), 58.32 (NCH2), 114.68 (ArC4), 117.73 (ArC5), 118.23 (ArC1), 123.09 (ArC6), 147.97 (ArC2—OH), 151.45 (ArC3—OCH3), 167.07 (C═N).

Synthesis of metalloligand [Ni(o-van-en)]·nH_2O (n = 1.17)

The synthesis was carried out according to the procedure described by Vráblová et al. (2019; 2020). Whereby solid H_2(*o-van-en*) (1 g, 3 mmol) and nickel(II) carbonate (0.350 g, 3 mmol) with 8 drops of Et_3N were added to 100 cm^3 of water and heated in an open beaker. After one and half hour brown microcrystalline product of nickel complex was separated by filtration, washed with 2 ml of ethanol and dried in air. Dry product was then used without further purification in the following syntheses of tetranuclear complexes. Yield: 75 %.

Anal. [%], calculated for $[Ni(o\text{-}van\text{-}en)]\cdot nH_2O$ (n = 1.5), $C_{18}H_{21}N_2O_{5.5}Ni$: C, 52.47; H, 5.14; N, 6.80; found: C, 51.91; H, 4.82; N, 6.47.

FT-IR [cm^{-1}]: 3508br, 3064w, 2943w, 2927w, 2829w, 1617s, 1603s, 1544s, 1470s, 1435s, 1401s, 1345s, 1313s, 1225s, 1166m, 1115m, 1092m, 1078m, 1001m, 969m, 865m, 852m, 781w, 733s, 665w, 619m, 564w, 544w, 482m, 430m, 408m.

^{1}H NMR [ppm]: 3.40s (6H), 3.69s (4H), 6.44d (2H), 6.77d (2H), 6.87d (2H), 7.87s (2H).

^{13}C NMR [ppm]: 55.49 (OCH3), 57.98 (NCH2), 113.52 (ArC4), 114.23 (ArC5), 120.25 (ArC1), 124.28 (ArC6), 150.46 (ArC2—OH), 155.37 (ArC3—OCH3), 162.68 (C═N).

Synthesis of [Ni(o-van-en)Dy(H_2O)$_2$(OH)]$_2$$Br_4$·6$H_2O$ (1) and [Ni(o-van-en)Dy(H_2O)$_2$(OH)]$_2$$Br_4$·2MeOH·2iPrOH·2$H_2O$ (2)

Metalloligand [Ni(*o-van-en*)] · *n*H_2O (0.148 g, 0.368 mmol) was dissolved in 15 mL of acetone; then, an acetonic solution (15 mL) of $DyBr_3$ in equimolar amount (0.152 g) was added. The reaction mixture was refluxed for 4 hours. Solid dark brown product of **1** was formed, filtered, and washed well with ethanol. Single crystal form of **1** was prepared by recrystallization using diffusion technique: solid product **1** (0.05 g, 0.03 mmol) was dissolved in methanol (5 mL) and the formed solution was layered with isopropanol (5 mL). After two weeks, brown prisms of **1** appeared in the closed vial system. Part of them was picked up from the mother liqueur and put under inert oil (Fomblin) due to low air stability and was later used for single crystal X-ray data collection. Most of the crystals formed were kept in the mother liquor and after six weeks of standing, these crystals (**2**) were once more checked using single crystal diffractometer; full X-ray data were collected at low temperature immediately after it was picked up from the liquid.

CHN analyses of single crystals were done after short time handling on air:

Anal. [%], calc. for (**1**), $C_{36}H_{58}N_4O_{20}Ni_2Dy_2Br_4$: C, 26.55; H, 3.59; N, 3.44; found: C, 26.42; H, 3.75; N, 3.12.

FT-IR [cm^{-1}] (**1**): 3460vw, 3261br, 2950w, 2850w, 1627s, 1610m, 1561w, 1470s, 1441m, 1410w, 1397w, 1348w, 1334w, 1301s, 1231s, 1170m, 1079s, 1054m, 1041m, 988m, 957m, 866m, 784m, 739s, 691w, 669w, 630w, 604w, 584w, 567w, 541w, 499w, 462m, 441s, 410s.

Anal. [%], calc. for (**2**), $C_{44}H_{74}N_4O_{20}Ni_2Dy_2Br_4$: C, 30.35; H, 4.28; N, 3.22; found: C, 29.66; H, 3.71; N, 3.34.

FT-IR [cm^{-1}] (**2**): 3251br, 2925w, 2848w, 1695vw, 1628s, 1611m, 1561w, 1472s, 1443m, 1403w, 1385w,

Tab. 2. Crystal data and structure refinement for **1** and **2**.

	1	**2**
Empirical formula	$C_{36}H_{58}N_4O_{20}Ni_2Dy_2Br_4$	$C_{44}H_{74}N_4O_{20}Ni_2Dy_2Br_4$
Molecular weight	1628.86	1741.13
Crystal system	Monoclinic	Monoclinic
Space group	$P\,2_1/c$	$P\,2_1/c$
Cell parameters		
a (Å)	10.3469(4)	11.6213(3)
b (Å)	20.4200(6)	21.5497(4)
c (Å)	12.2597(3)	11.8925(2)
α (°)	90	90
β (°)	91.950(3)	96.330(2)
γ (°)	90	90
V (Å^3)	2588.78(14)	2960.15(11)
Z	4	2
D_{calc} (Mg · m^{-3})	2.090	1.953
Abs. coeff. (mm^{-1})	20.254	17.762
Crystal color, form	brown prism	brown prism
Crystal size (mm)	0.232 × 0.149 × 0.092	0.247 × 0.168 × 0.147
T (K)	100(2)	100(2)
Radiation λ (Å)	1.54184	1.54184
θ range (°)	4.208–67.491	3.827–67.494
Index ranges	$-12 \le h \le 12$	$-13 \le h \le 13$
	$-24 \le k \le 24$	$-19 \le k \le 25$
	$-14 \le l \le 14$	$-14 \le l \le 14$
Refl. coll./ indep.	19633 / 4653	21626 / 5326
Goodness-of-fit (F^2)	1.138	1.040
Final R indices	$R1$ = 0.0652,	$R1$ = 0.0722
($I > 2\sigma(I)$)	$wR2$ = 0.1824	$wR2$ = 0.1832
R indices (all data)	$R1$ = 0.0738,	$R1$ = 0.0772
	w$R2$ = 0.1948	$wR2$ = 0.1883
Diff. peak and hole (e · Å^{-3})	–2.81, 3.60	–2.56, 1.98

1334w, 1302s, 1230, 1169m, 1127w, 1110w, 1079s, 1055w, 1023m, 989m, 987w, 955m, 865m, 851w, 818w, 779w, 737s, 689w, 668w, 627w, 605w, 582w, 568w, 541m, 499w, 478w, 462m, 440s, 411s.

Physical measurements

CHN analyses were measured using a CHNOS elemental analyzer Vario MICRO cube instrument (Elementar Analysensysteme GmbH). IR spectra in the 400—4000 cm^{-1} range were recorded on a Nicolet 6700 FT-IR spectrophotometer (Thermo Scientific) using the ATR method. ^{1}H and ^{13}C NMR spectra of H_2(*o-van-en*) ligand were measured in DMSO-d6 solution using a Varian VNMRS 600 spectrometer with an Oxford superconducting magnet (14.09 T, 54 mm bore).

X-ray crystallography

Single crystal X-ray measurements of title complexes **1** and **2** were performed using a Rigaku XtaLAB Synergy S diffractometer equipped with microfocus CuKα radiation and a Hybrid Pixel Array Detector (HyPix-6000HE). An Oxford Cryosystems (Cryostream 800) cooling device was used for data collection at 100 K. CrysAlisPro software was used for data collection, cell refinement, and data reduction (Oxford Diffr., 2022). Data were corrected for absorption effects using empirical absorption correction (spherical harmonics), implemented in the SCALE3 ABSPACK scaling algorithm, and analytical numeric absorption correction using a multifaceted crystal model with CrysAlisPro software (Blessing, 1995). Crystal structures were solved and refined using the SHELXT (Sheldrick, 2015a) and the SHELXL (Sheldrick, 2015b) programs. All non-hydrogen atoms were refined anisotropically. Hydrogen atoms bonded to carbon atoms were placed in calculated positions and refined using a riding model with isotropic thermal parameters tied to their respective parent atoms: $U_{iso}(H) = 1.2\,U_{eq}(C)$ for non-methyl H atoms, and $U_{iso}(H) = 1.5\,U_{eq}(C)$ for methyl groups. Hydrogen atoms bound to oxygen atoms of water and alcoholic molecules were found in the difference map; their isotropic thermal parameters were tied with the parent O atoms ($U_{iso}(H) = 1.5\,U_{eq}(O)$). During refinement, the O—H bond distances were restrained using the DFIX command. In the structure of **2**, the ethylenediamine fragment is disordered over two positions with respective refined site occupation factors 0.50(4)/0.50(4) (C9A, C10A / C9B, C10B). Structural figures were drawn using the Diamond program (Brandenburg and Putz, 2022). Geometric parameters were also calculated using the PLATON program (Spek, 2003). Program Mercury CSD 4.2.0 (Macrae et al., 2020) was used to compare molecular structures. Crystal data and final parameters of the structure refinement are summarized in Table 2, while selected geometric parameters are given in Table 3. Possible hydrogen bonds are gathered in Tables 4 and 5.

Results and discussion

Two new tetranuclear complexes [Ni(*o-van-en*)$Dy(H_2O)_2(OH)]_2Br_4 \cdot 6H_2O$ (**1**) and [Ni(*o-van-en*)$Dy(H_2O)_2(OH)]_2Br_4 \cdot 2MeOH \cdot 2\,iPrOH \cdot 2H_2O$ (**2**) were prepared in a single crystal form from a system consisting of metalloligand [Ni(*o-van-en*)] and $DyBr_3$ using the diffusion method. First, single crystals of **1** formed by recrystallization of the bulk sample while long-time standing of crystals **1** in the mother liquor in the presence of isopropanol led to their transformation to new single crystals **2**. While solvent molecules in complex **1** comprise only water, in complex **2**, methanol and isopropanol also act as solvent molecules alongside water. As the complexes differ in the solvent molecules' content, they can be considered as solvatomorphs (Brittain, 2009). Solvatomorphism is not an uncommon phenomenon, e.g. it was observed in case of $\{[Mn(cyclam)][Fe(CN)_6]\cdot nH_2O\}_n$ (Nowicka, 2017) or $[Cu(ClO_4)_2(LH)_4] \cdot x$(solvent) (*L*H = 5-phenylimidazole) (Loukopoulos et al., 2014), various solvatomorphs of the metalloligand alone have also been studied (Vráblová et al., 2020). Analogous tetranuclear complexes have already been reported, e.g. $[Ni_2Dy_2(L)_2(o\text{-van})_2(CO_3)_2(NO_3)_2(MeOH)_2]$ (H*L* = 2-methoxy-6-[(E)-phenyliminomethyl] phenol; GACQUZ) (Upadhyay et al., 2016), and $[(\mu_4\text{-}CO_3)_2\{Ni(3\text{-}MeOsaltn)(MeOH)Dy(NO_3)\}_2]$ (3-MeOsaltn = *N,N´*-bis(3-methoxy-2-oxybenzylidene)-1,3-propanediaminato; WIMDUT) (Sakamoto et al., 2013) (Table 1). On the other hand, the present two complexes are the first examples in which bromide anions are present as anions.

Complexes **1** and **2** were characterized using IR spectroscopy with typical absorption bands being ν(C═N) vibrations of imine groups from the deprotonated Schiff base ligand (Horák and Papoušek, 1976; Nakamoto, 2009); these were observed at 1627 and 1628 cm^{-1} for **1** and **2**, respectively (Fig. 1). These values are in good agreement with the results reported by Liu et al. (2017) for analogous tetranuclear Ni(II)/Dy(III) complexes as well as for similar dinuclear bromido complexes (Krešáková et al., 2025). Weak but characteristic absorption bands found slightly above 3000 cm^{-1} and slightly below 3000 cm^{-1} were assigned to the $\nu(C_{ar}—H)$ and $\nu(C_{al}—H)$ stretching vibrations, respectively. The broad absorption bands centered at 3261 cm^{-1} (**1**) and 3251 cm^{-1} (**2**) correspond to the ν(O—H)

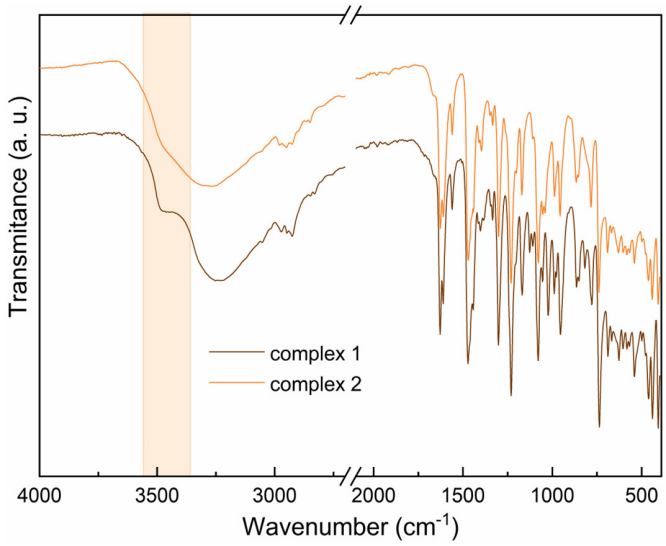

Fig. 1. IR spectra of complexes **1** (brown line) and **2** (orange line).

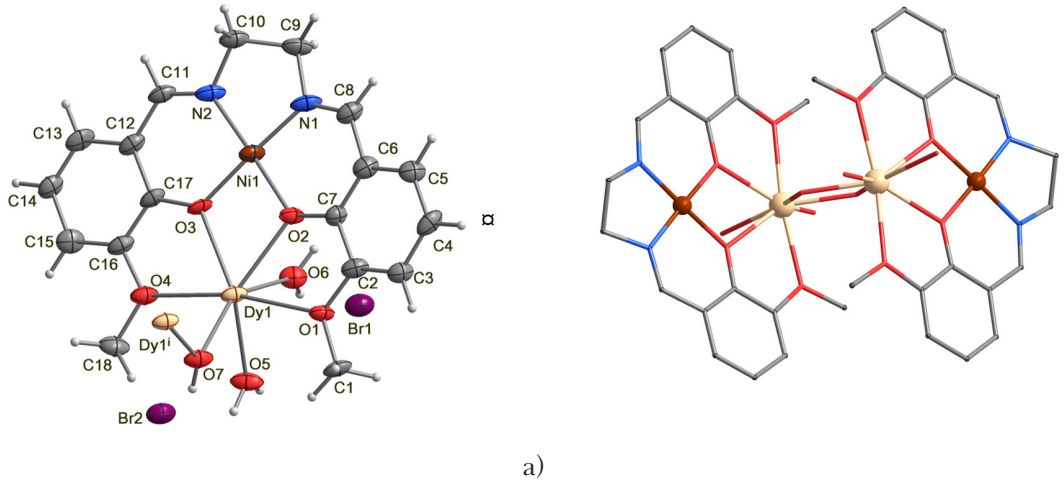

a)

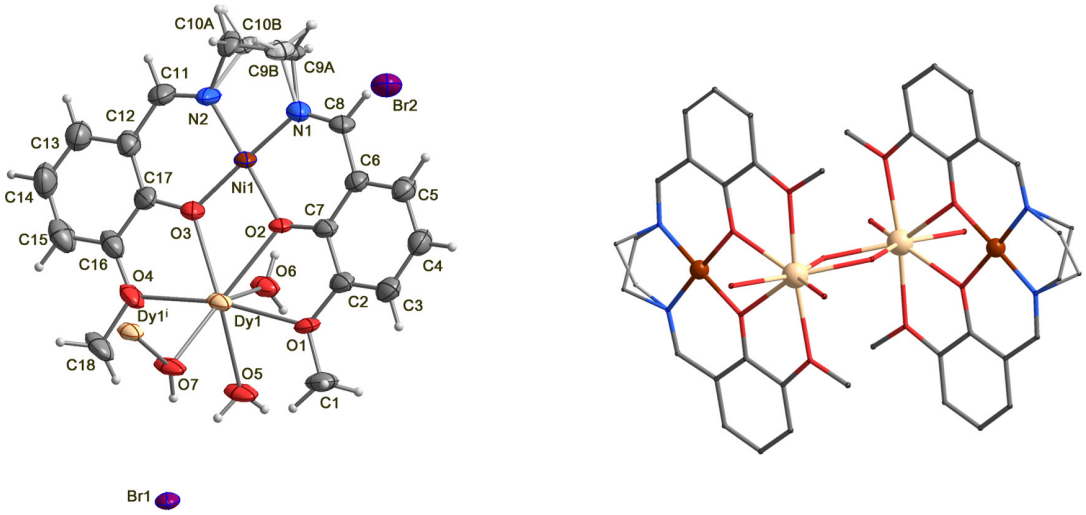

b)

Fig. 2. a), b) left: Asymmetric unit of **1** (a) and **2** (b) with atom numbering scheme. Thermal ellipsoids are drawn at the 50 % probability level (solvate molecules are omitted for clarity).
a), b) right: Tetranuclear Ni_2Dy_2 complex cation in **1** (a) and in **2** (b); Ni(II) atoms are depicted as brown balls, Dy(III) atoms as light orange balls, and nitrogen (blue), oxygen (red), carbon (grey) atoms are drawn in wire model (hydrogen atoms and solvate molecules are omitted for clarity).

vibrations of water (and methanol/isopropanol in **2**) solvate molecules. Another significant sharp absorption band at 1079 cm^{-1} in both spectra was assigned to ν(C—O) valence vibration located on the aromatic ring of the bicompartmental Schiff base ligand.

Crystal structures

Both complexes $[Ni(o\text{-}van\text{-}en)Dy(H_2O)_2(OH)]_2Br_4 \cdot 6H_2O$ (**1**) and $[Ni(o\text{-}van\text{-}en)Dy(H_2O)_2(OH)]_2Br_4 \cdot 2i$PrOH $\cdot$ 2MeOH $\cdot$ $2H_2O$ (**2**) have ionic structure composed of the same centrosymmetric $\{Ni^{II}/Dy^{III}\}_2$ tetranuclear complex cations $[\{Ni(o\text{-}van\text{-}en)Dy(H_2O)_2(OH)\}_2]^{4+}$ and bromide anions; the only compositional difference is in the amount and quality of solvate molecules in **1** and **2** (Fig. 2). While in the structure of **1**, only water solvate molecules are present, in the structure of **2**, molecules of methanol and isopropanol besides water molecules are visible (Fig. 2a, b left). Each fully deprotonated ligand acts as a multidentate linker holding two different metal ions: Ni(II) occupies the cis-N_2O_2 site to fulfill a square configuration, whereas the heavier Dy(III) is held by the O_8 pocket; among these eight oxygen atoms, four are provided by the $(o\text{-}van\text{-}en)^{2-}$ ligand. The Ni(II) and Dy(III) atoms are linked by a pair of monoatomic O-bridges and therefore are in proximity with respective distances Ni···Dy of 3.3888(15) Å in **1** and 3.4152(12) Å in **2**. The two dinuclear units $\{Ni(o\text{-}van\text{-}en)Dy(H_2O)_2\}$ are further linked by a pair of μ-hydroxy bridges between the neighbouring Dy(III) atoms yielding a $\{Dy(\mu\text{-}OH)_2Dy\}$ core and resulting in the formation of the tetranuclear complex cation $[\{Ni(o\text{-}van\text{-}en)Dy(H_2O)_2(\mu\text{-}OH)\}_2]^{4+}$. Within this $\{Dy(\mu\text{-}OH)_2Dy\}$ core, the neighbouring Dy(III) atoms are at distance Dy1···Dy1^i (i: 1 – *x*, 1 – *y*, 1 – *z*) of 3.7195(7) Å in **1** and 3.7310(6) Å in **2** (i: 1 – *x*, 1 – *y*, 2 – *z*). The last two oxygen atoms are from the coordinated aqua ligands (Fig. 2a, b left). The coordination polyhedra of the Dy(III) atom in both **1** and **2**, based on the calculations using the SHAPE program (Llunell et al., 2013), can be described as a trigonal dodecahedron (Fig. 3).

The formation of such tetranuclear complex cations from originally dinuclear ones can be explained by the condensation process (Thompson, 2002; Jiang et al., 2017). A similar tetranuclear cluster $[\{Cu_2L(\mu_{1,1}\text{-}N_3)(ClO_4)\}_2(\mu_{1,3}\text{-}N_3)_2]$ (UZUXOD) (Majumder et al., 2011) is a result of the interlinking of two dicopper(II) units $[Cu_2L(\mu_{1,1}\text{-}N_3)(ClO_4)]^+$ by two end-to-end bridging azide anions. H*L* is a compartmental ligand which is the 1/2 condensation product of 2,6-diformyl-4-ethylphenol and 2-(2-aminoethyl)pyridine (Majumder et al., 2011).

A search in CSD (Groom et al., 2016) showed only six structures based on $\{NiO_2DyO_2DyO_2Ni\}$ core reported up to now (see Table 1). Structures of **1** and **2** show dimeric tetranuclear complex cations $[\{Ni(o\text{-}van\text{-}en)Dy(H_2O)_2(OH)\}_2]^{4+}$ containing the basic fragment $[NiO_2DyO_2DyO_2Ni]$ with a linear arrangement of Ni···Dy···Dy···Ni central atoms. It is noteworthy that Ni(II) atoms are diamagnetic. Similar atomic environments of Dy(III) atoms were found in another polynuclear complex $[Ni_2(L)DyCl(OH)(MeO)(MeOH)_3]_2Cl_2(ClO_4)_2 \cdot MeOH$ (HOBQUM; H_2L=*N,N´*-bis(3-methoxysalicylidene) diethylenetriamine) (Zhao et al., 2014); except that the octa-coordination of Dy(III) is also present with the double OH bridge. Analogous tetranuclear complex $[(\mu_3\text{-}CO_3)_2\{Ni(HL)(EtOH)Dy(CH_3COO)\}_2] \cdot 2EtOH$ (JASTUV01; H_3L = H_3L = *N,N´*-bis(3-methoxysalicylidene)-1,3-diamino-2-propanol) (Jiang et al., 2017) was found; Dy(III) central atom is octa-coordinated with distorted triangular dodecahedral geometry.

Dy1 and Dy1^i (i: 1 – *x*, 1 – *y*, 1 – *z* (**1**); i: 1 – *x*, 1 – *y*, 2 – *z* (**2**)) are doubly bridged by O atoms of hydroxy groups to form a Dy_2O_2 rhombus with angles of 112.2(3)° (**1**) (112.8(2)° (**2**)) and 67.8(3)° (**1**) (67.2(2)° (**2**)) for Dy—O—Dy and O—Dy—O, respectively. Ni—O and Ni—N bond lengths

a) b)

Fig. 3. Coordination polyhedra of Dy(III) atoms in **1** (a) (symmetry code: **i:** 1 – *x*, 1 – *y*, 1 – *z*); and in **2** (b) (symmetry code: **i:** 1 – *x*, 1 – *y*, 2 – *z*).

cover ranges of 1.828(8)–1.851(1) Å for structure **1** and 1.826(6)–1.860(5) Å for structure **2**. These values are in good agreement with analogous Ni(II)/Ln(III) complexes (Krešáková et al., 2025; Vráblová et al. 2019). On the contrary, Dy—O distances are in the range of 2.210(6)–2.500(6) Å for **1** and 2.249(5)–2.492(7) Å for **2** (see Tab. 3). Similar Dy—O values were observed also in related complexes (Wu et al., 2017).

The presence of both coordinated and solvated water molecules in both **1** and **2**, along with additional solvate molecules of methanol and isopropanol found in sample **2**, leads to distinct supramolecular structures of **1** and **2**. A list of potential hydrogen bonds of O—H···O type and possible weak hydrogen bonding interactions of O—H···Br type is provided in Tabs. 4 and 5, respectively. It is important to highlight that one hydrogen atom (H92) from the solvate water molecule (O9) in compound **1** does not engage in the hydrogen bonding network (Fig. 4). The IR spectrum of **1** shows a medium absorption band at 3460 cm^{-1}, which can be attributed to O—H stretching vibrations likely originating from water molecules not involved in extensive hydrogen bonding (see Fig. 1, highlighted area). However, in both spectra, shoulders are centered around 3300 cm^{-1}, which can be explained by OH stretching vibrations of the binding OH groups (Ferraro et al., 1965). Thus, the more pronounced shape of the shoulder in the spectrum of **1** can be ascribed to the water molecule.

Stacking π-π intermolecular interactions of the aromatic rings of the compartmental Schiff base-type ligand also contribute to the stability of the supramolecular structure. Distances of centroids *Cg*1···*Cg*1^{iii} (iii: 1 – *x*, 1 – *y*, – *z* (**1**); iii: *x*, *y*, 1 + *z* (**2**)) are 3.6181(1) for **1** and 3.5322(1) Å for **2**. Consequently, within the structure of both **1** and **2**, a topologically chain-like arrangement of closely positioned dimeric units of tetranuclear complexes running along the *c*-axis is formed (Figs. 4, 5). Unit chains are connected through hydrogen bonding systems, which leads to the formation of a final three-dimensional crystal structure.

Tab. 3. Selected bond lengths and angles [Å, °] for **1** and **2**.

	1	**2**		**1**	**2**
Ni1—N1	1.829(8)	1.826(6)	Dy1—O4	2.500(6)	2.492(7)
Ni1—N2	1.840(8)	1.830(6)	Dy1—O5	2.398(6)	2.415(5)
Ni1—O2	1.851(6)	1.860(5)	Dy1—O6	2.406(6)	2.342(5)
Ni1—O3	1.848(6)	1.845(5)	Dy1—O7	2.210(6)	2.231(5)
Dy1—O1	2.454(6)	2.487(5)	Dy1—O7^{i}	2.271(6)	2.249(5)
Dy1—O2	2.347(6)	2.362(5)	Dy1—O7—Dy1^{i}	112.2(3)	112.8(2)
Dy1—O3	2.362(5)	2.360(5)	O7—Dy1—O7^{i}	67.8(3)	67.2(2)

Symmetry codes: **i:** 1 – *x*, 1 – *y*, 1 – *z* (**1**); **i:** 1 – *x*, 1 – *y*, 2 – *z* (**2**).

Tab. 4. Potential hydrogen bonding interactions in **1** [Å, °].

D—H···A	***d*(D—H)**	***d*(H···A)**	***d*(D···A)**	**<(DHA)**	
O5—H51···O8	0.84(2)	1.92(3)	2.759(9)	173(12)	
O5—H52···Br2^{ii}	0.84(2)	2.44(4)	3.287(6)	163(11)	
O6—H61···O9	0.841(10)	1.93(3)	2.748(10)	165(10)	
O6—H62···Br1	0.840(10)	2.49	3.243(6)	150(8)	
O7—H7···Br2^{ii}	0.84	2.63	3.370(6)	147.9	
O8—H81···Br1	0.840(10)	2.48(3)	3.313(7)	169(11)	
O8—H82···Br2	0.840(10)	2.43(3)	3.252(7)	166(9)	
O9—H91···O10^{vi}	0.840(10)	2.00(4)	2.807(10)	162(13)	
O10—H101···Br1^{iii}	0.840(10)	2.74(11)	3.355(8)	132(12)	
O10^{iii}—H102^{iii}···O8^{v}	0.841(10)	2.12(4)	2.950(10)	167(14)	
π-π	***Cg*···*Cg***	**α**	**β**	**γ**	**Slippage**
*Cg*1···*Cg*1^{iii}	3.6181(1)	0	23.4	23.4	1.435

Symmetry codes: **i:** 1 – *x*, 1 – *y*, 1 – *z*; **ii:** *x*, 3/2 – *y*, 1/2 + *z*; **iii:** 1 – *x*, 1 – *y*, –*z*; **iv:** *x*, *y*, –1 + *z*; **v:** *x*, 3/2 – *y*, –1/2 + *z*; **vi:** –1 + *x*, *y*, *z*. Centroid *Cg*1 is the center of gravity of a six-membered ring C12-C17.

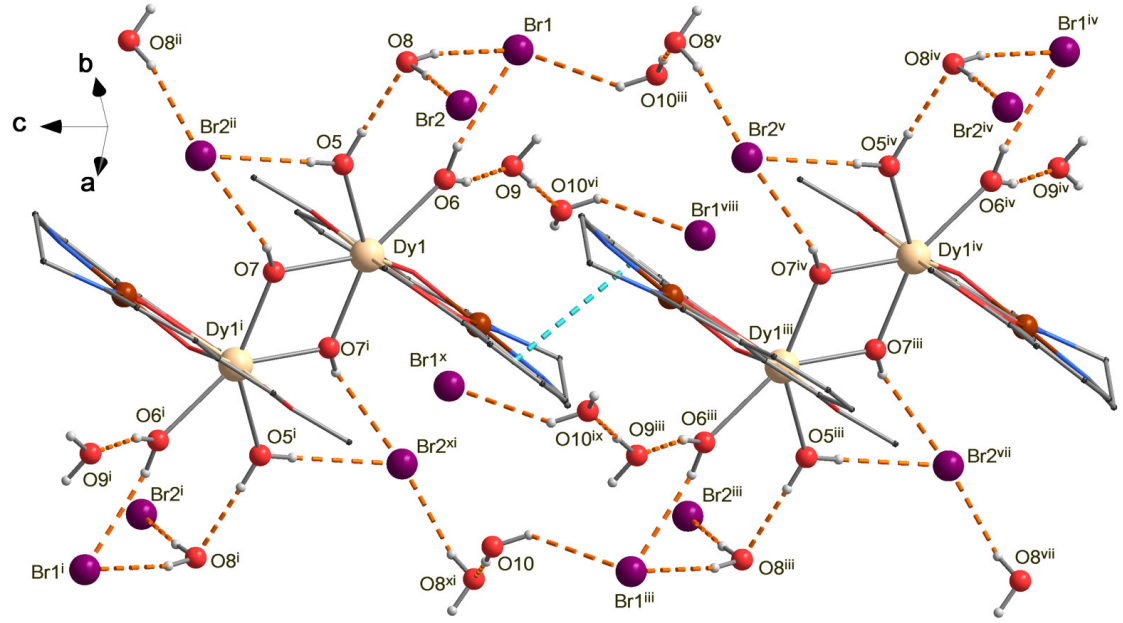

Fig. 4. View of potential hydrogen bonding system in **1** indicating chain-like arrangement of dimers of the Ni_2Dy_2 units. All atoms non-relevant for the hydrogen bonding system are omitted for clarity. Potential hydrogen bonding interactions are drawn as orange dashed lines and π-π interactions are shown as blue dashed lines.

Symmetry codes: **i:** 1 – *x*, 1 – *y*, 1 – *z*; **ii:** *x*, 3/2 – *y*, 1/2 + *z*; **iii:** 1 – *x*, 1 – *y*, –*z*; **iv:** *x*, *y*, –1 + *z*; **v:** *x*, 3/2 – *y*, –1/2 + *z*; **vi:** –1 + *x*, *y*, *z*; **vii:** 1 – *x*, –1/2 + *y*, –1/2 – *z*; **viii:** –x, 1 – *y*, –*z*; **ix:** 2 – *x*, 1 – *y*, –*z*; **x:** 1 + *x*, *y*, *z*; **xi:** 1 –*x*, –1/2 + *y*, 1/2 – *z*.

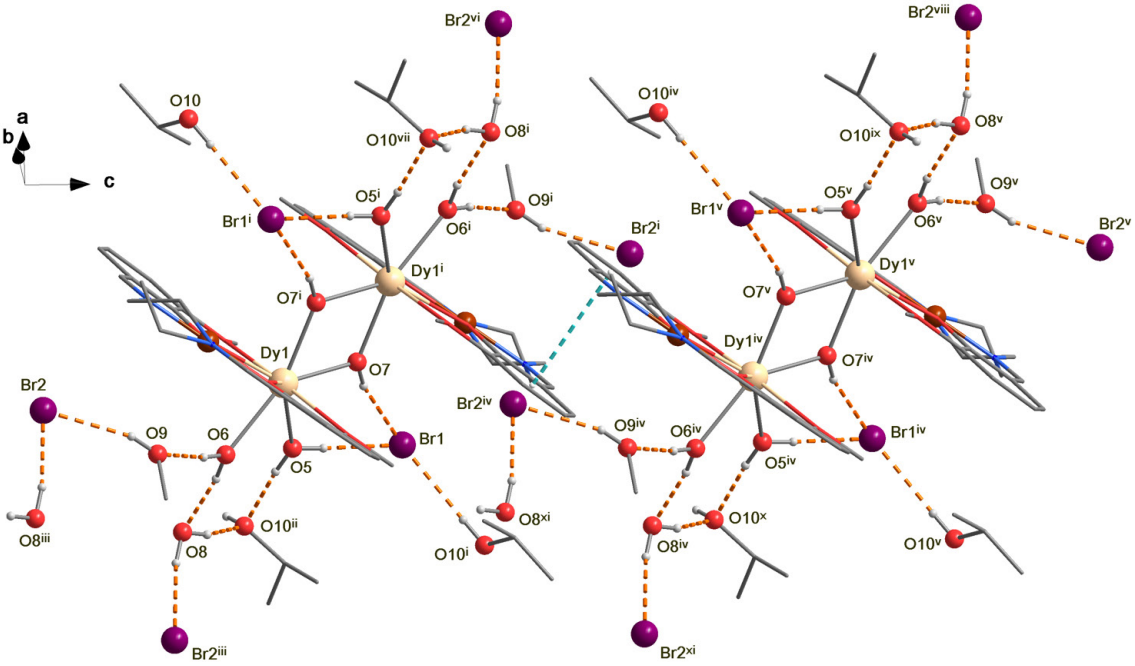

Fig. 5. View of potential hydrogen bonding system in **2** indicating chain-like arrangement of dimers of the Ni_2Dy_2 units. All atoms non-relevant for the hydrogen bonding system are omitted for clarity. Potential hydrogen bonding interactions are drawn as orange dashed lines and π-π interactions are shown as blue dashed lines.

Symmetry codes: **i:** 1 – *x*, 1 – *y*, 2 – *z*; **ii:** 1 – *x*, 1/2 + *y*, 3/2 – *z*; **iii:** *x*, *y*, 1 + *z*; **iv:** –*x*, 1 – *y*, 1 – *z*; **v:** 1 – *x*, 1 – *y*, 3 + *z*; **vi:** 1 + *x*, *y*, 1 + *z*; **vii:** *x*, 3/2 – *y*, 1/2 + *z*; **viii:** 1 + x, *y*, 2 + *z*; **ix:** *x*, 3/2 – *y*, 3/2 + *z*; **x:** 1 – *x*, –1/2 + *y*, 5/2 – *z*; **xi:** –*x*, –1 – *y*, 2 – *z*.

Tab. 5. Potential hydrogen bonding interactions in **2** [Å, °].

D—H···A	***d*(D—H)**	***d*(H···A)**	***d*(D···A)**	**<(DHA)**
O5—H51···Br1	0.85(2)	2.42(3)	3.259(6)	173(12)
O5—H52···O10^{ii}	0.84(2)	1.94(3)	2.771(8)	170(9)
O6—H61···O8	0.84(2)	1.82(3)	2.658(8)	173(9)
O6—H62···O9	0.85(2)	1.83(2)	2.678(8)	175(12)
O7—H7···Br1	0.84	2.54	3.358(5)	166.4
O8—H81···Br2^{iv}	0.84(2)	2.41(4)	3.233(7)	166(13)
O8—H82···O10^{ii}	0.84(2)	2.02(6)	2.778(9)	150(12)
O9—H91···Br2	0.84	2.40	3.209(7)	163.1
O10—H101···Br1^{i}	0.84	2.42	3.262(6)	177.8

π-π	***Cg*···*Cg***	**α**	**β**	**γ**	**Slippage**
*Cg*1···*Cg*1^{iii}	3.5322(1)	0	9.1	9.1	0.560

Symmetry codes: **i:** 1 – *x*, 1 – *y*, 2 – *z*; **ii:** 1 – *x*, 1/2 + *y*, 3/2 – *z*; **iii:** *x*, *y*, 1 + *z*; **iv:** –*x*, 1 – *y*, 1 – *z*. Centroid *Cg*1 is the center of gravity of a six-membered ring C2-C7.

Conclusion

Two novel tetranuclear 3*d*/4*f* complexes were prepared and spectroscopically and structurally characterized. Both complexes, **1** and **2**, exhibit ionic structures built up of bromide anions and tetranuclear $[\{Ni(o\text{-}van\text{-}en)Dy(H_2O)_2(OH)\}_2]^{4+}$ complex cations. In addition, **1** and **2** contain water and methanol/isopropanol/water solvate molecules, respectively, i.e. these complexes are solvatomorphs. The complex cation contains a $[NiO_2DyO_2DyO_2Ni]$ core with Ni-Dy-Dy-Ni linear arrangement of central atoms. The rich system of hydrogen bonding interactions was elucidated based on the presence of various solvent molecules using crystal structure determination.

Acknowledgement

This work was supported by Grant 09I03-03-V04-00176 (project name: Hybrid materials formed of layered aluminosilicates and molecular magnets – HERCULES) financed by the EU/NextGenerationEU/ program "Recovery and Resilience Plan, part of Investment 3: Excellent Science". We would like to thank Dr. Miroslava Litecká from the Department of Materials Chemistry at the Czech Academy of Sciences for gathering X-ray single crystal data.

Appendix A. Supplementary data

Crystallographic data for compounds 1 and 2 are deposited in the Cambridge Crystallographic Data Centre, CCDC no. 2464566 and 2464568, respectively. These data can be obtained free of charge via http://www.ccdc.cam.ac.uk/conts/retrieving.html, or from the Cambridge Crystallographic Data Centre, 12 Union Road, Cambridge CB2 1EZ, UK; fax: (+44) 1223-336-033; or e-mail: deposit@ccdc.cam.ac.uk.

References

Andruh M (2015) Dalton Trans. 44: 16633–16653.

Blessing RH (1995) Acta Cryst. B51: 816–823.

Brandenburg K, Putz H (2022) Program DIAMOND (version 4.6.8) Crystal Impact GbR., Bonn, Germany.

Brittain HG (2009) Polymorphism in Pharmaceutical Solids, 2nd Ed., Informa Healthcare USA, Inc.

CrysAlisPRO (version 1.0.43) (2022) Rigaku Oxford Diffraction, Yarnton, UK.

Cristovao B, Miroslaw B, Klak J, Rams M (2015) Polyhedron 86: 697–704.

Ferraro JR, Walker WR (1965) Inorg. Chem. 4(10): 1382–1386.

Groom CR, Bruno IJ, Lightfoot MP, Ward SC (2016) The Cambridge Structural Database, Acta Crystallogr. B 72: 171–179.

Hardy EE, Wyss KM, Gorden JD, Ariyarathna IR, Miliordos E, Gorden AEV (2017) Chem. Commun. 53: 11984–11987.

Horák M, Papoušek D (1976) Infračervená spektra a struktura molekul. Academia, Praha. ISBN 509-21-857.

Chandrasekhar V, Hossain S, Das S, Sutter J-P (2013) Inorg. Chem. 52: 6346–6353.

Jiang L, Liu Y, Liu X, Tian J, Yan S (2017) Dalton Trans. 46: 12558–12573.

Krešáková L, Litecká M, Oyarzabal I, Titiš J, Červeňáková M, Hillard EA, Robert J, Černák J (2024) New J. Chem. 48: 17750–17760.

Krešáková L, Miño A, Kuchár J, Smolko R, Černák J (2025) J. Coord. Chem. 78: 1930–1948.

Langley SK, Chilton NF, Moubaraki B, Murray K (2013) Chem. Commun. 49: 6965–6967.

Langley SK, Le C, Ungur L, Moubaraki B, Abrahams BF, Chibotaru LF, Murray KS (2015) Inorg Chem. 54: 3631–3642.

Liu Y-A, Wang C-Y, Zhang M, Song X-Q (2017) Polyhedron 122: 278–286.

Llunell M, Casanova D, Cirera J, Alemany P, Alvarez S (2013) SHAPE Program for the Stereochemical Analysis of Molecular Fragments by Means of

Continuous Shape Measures and Associated Tools, Version 2.1 (2013). Universitat de Barcelona, Barcelona, Spain.
Loukopoulos E, Papatriantafyllopoulou C, Moushi E, Kitos AA, Tasiopoulos AJ, Perlepes SP, Nastopoulos V (2024) Acta Crystallogr. B Struct. Sci. Cryst. Eng. Mater. 80: 347–359.
Macrae CF, Sovago I, Cottrell SJ, Galek PTA, McCabe P, Pidcock E, Platings M, Shields GP, Stevens JS, Towler M, Wood PA (2020) J. Appl. Cryst. 53: 226–235.
Majumder S, Sarkar S, Sasmal S, Sanudo EC, Mohanta S (2011) Inorg. Chem. 50: 7540–7554.
Nakamoto K (2009) Infrared and Raman Spectra of Inorganic and Coordination Compound, 6th Edition, J. Wiley & Sons, New York.
Nowicka B, Heczko M, Rams M, Reczyński M, Gaweł B, Nitek W, Sieklucka B (2017) Eur. J. Inorg. Chem. 1: 99–106.
Sheldrick GM (2015a) Acta Crystallogr. A 71: 3–8.
Sheldrick GM (2015b) Acta Crystallogr. C 71: 3–8.
Sakamoto S, Fujinami T, Nishi K, Matsumoto N, Mochida N, Ishida T, Sunatsuki Y, Re N (2013) Inorg. Chem. 52: 7218–7229.
Spackman PR, Turner MJ, McKinnon JJ, Wolff SK, Grimwood DJ, Jayatilaka D, Spackman MA (2021) J. Appl. Cryst. 54: 1006–1011.
Thompson LK (2002) Coord. Chem. Rev. 233-234: 193–206.
Tsantis ST, Lagou-Rekka A, Konadaris KF, Raptopoulou CP, Bekiari V, Psycharis V, Perlepes SP (2019) Dalton Trans. 48: 15668–15678.
Upadhyay A, Das C, Langley SK, Murray KS, Srivastava AK, Shanmugam M (2016) Dalton Trans. 45: 3616–3626.
Vignesh KR, Langley SK, Murray KS, Rajaraman G (2017) Inorg. Chem. 56: 2518–2532.
Vráblová A, Tomás M, Falvello LR, Dlháň Ľ, Titiš J, Černák J, Boča R (2019) Dalton Trans. 48: 13943–13952.
Vráblová A, Tomás M, Titiš J, Černák J, Falvello LR (2020) Inorg. Chim. Acta 512: 119874.
Wu H, Li M, Zhang S, Ke H, Zhang Y, Zhuang G, Wang W, Wei Q, Xie G, Chen S (2017) Inorg. Chem. 56: 11387–11397.
Zhao L, Wu J, Ke H, Tang J (2014) Inorg. Chem. 53: 3519–3525.